Nucleic Acids Research, 1999, Vol. 27, No. 8 **1943–1949**

Ethanol-induced structural transitions of DNA on mica

Ye Fang, Thomas S. Spisz[1] and Jan H. Hoh*

Department of Physiology, Johns Hopkins University School of Medicine, 725 N. Wolfe Street, Baltimore, MD 21205, USA and [1]Applied Physics Laboratory, Johns Hopkins University, Johns Hopkins Road, Laurel, MD 20723, USA

Received September 22, 1998; Revised February 18,1999; Accepted March 1, 1999

ABSTRACT

The effect of ethanol on the structure of DNA confined to mica in the presence of Mg^{2+} was examined by varying the ethanol concentration and imaging the DNA by atomic force microscopy. Contour length measurements of the DNA show a transition from all-B-form at 0% ethanol to all-A-form at >25% ethanol. At intermediate ethanol concentrations, contour lengths suggest that individual molecules of air-dried DNA are trapped with mixed compositions of A-form and B-form. The relative composition depends on the ethanol concentration. Fitting the length distributions at intermediate ethanol concentrations to a simple binomial model results in an upper bound estimate for the A-form and B-form domains of ~54 bp in the individual molecules. In addition to length changes, the apparent persistence length of DNA decreases with increasing ethanol concentration. At high concentrations of ethanol (>20%), DNA formed several higher order structures, including flower shaped condensates and toroids.

INTRODUCTION

Double helical DNA adopts conformations ranging from right-handed A-, B- or C-forms to left-handed Z-form, depending on sequence and nucleotide composition, environment and overall topology of the DNA (1). Changes in the environment such as solvent and counterions can result in various transformations between those conformations. A specific example is that the introduction of ethanol into a DNA solution can alter DNA conformation from B-form to A- or C-form, depending on the nature of the counterion (2–6). It has been shown that ~80% ethanol is required for a complete B-to-A transition of a DNA in the presence of cations such as Na^+, K^+ or Cs^+ (5). In contrast, the presence of the strongly hydrated counterion Mg^{2+} is found to prevent the formation of the A-form, as ethanol concentration increases (6). The B–A transition is also sequence dependent, and the transition starts at so-called A-form-philic tracts that contain CC/GG contacts, and proceeds cooperatively within individual DNA molecules, as the water activity continuously decreases (7–9). The characteristic size of the A-form and B-form domains during the B–A transition is estimated to be 10–30 bp (2,7,8). Ethanol can also participate in the formation of higher ordered DNA structures, such as supercoiled and toroidal forms (1,10). The toroid formation can occur in the presence (11,12) or absence (13–15) of multivalent cations.

The structure of DNA adsorbed to solid surfaces has been studied to understand the nature of DNA–surface interactions, or because the adsorbed structures may shed light on the structure in solution. For example, the interaction of DNA with a membrane surface is important for transfection systems based on cationic lipids (16–18), and DNA condensation and decondensation *in vivo* is also thought to involve surfaces (19–21). The solution structure of kinked (22–23), supercoiled (24), bent (25) and looped (26) DNA molecules has been inferred from those of DNA adsorbed on surfaces. Atomic force microscopy (AFM) has become a useful tool for examining DNA confined to surfaces, in part because it expands the types of surfaces and environments that can be used. Transmission electron microscopy is limited to thin electron translucent surfaces such as amorphous carbon or formvar, and can only be used with the sample in vacuum or embedded in ice. AFM, on the other hand, can be used to visualize the structure of DNA molecules with surfaces such as mica (27), silicon (28), lipid bilayers (16–17), self-assembled monolayers (28,29), amorphous carbon (30) and sapphire (31), in ambient, low pressure or aqueous environments (32,33). Here we report on the structure of DNA confined to a mica surface in the presence of varying concentrations of ethanol. In agreement with the previous observation by Courey *et al.* (34), we find that DNA on mica is completely converted from B-form to A-form DNA at 25% ethanol. In addition, we find that molecules with varying composition of A-form and B-form DNA can be trapped at ethanol concentrations between 0 and 20%. At higher ethanol concentrations several well-defined structures appear, including flowers and toroids that are similar to those previously reported in the spermidine-induced DNA condensation (10,35).

MATERIALS AND METHODS

DNA and chemicals

Plasmid pSP64 poly(A) of 3033 bp (Boehringer Mannheim, Indianapolis, IN) was linearized by complete digestion with the *Sca*I endonuclease (Boehringer Mannheim). A linear DNA of 1968 bp was generated from a pUC19 derivative. A linear DNA of 672 bp was generated by double digestion of pTZ19R (Sigma Chemical Company, St Louis, MO) by *Sca*I and *Dra*I (Boehringer Mannheim). DNA fragments were purified using Gene Clean (Bio101, Vista, CA) and precipitated with ethanol. The DNA pellets obtained were re-suspended in Millipore purified water (>18 MΩ-cm^{-1}; MilliQ-UV, Millipore Co., Bedford, MA) and stored at –20°C. DNA concentration was determined by the absorption at 260 nm. Salts and ethanol of 100% were used as received (Sigma Chemical Co.).

*To whom correspondence should be addressed. Tel: +1 410 614 3795; Fax: +1 410 614 3797; Email: jan.hoh@jhu.edu

Sample preparation

Nine millimeter diameter disks of ruby muscovite mica (grade V1-V2; Asheville-Schoomaker Mica Co., Newport News, VA), each attached to a magnetic steel disk, were used as substrates for DNA adsorption. For non-trapping conditions, experiments were performed by mixing 50 µl of a 1 nM DNA solution containing 10 mM $MgCl_2$ and a 50 µl ethanol solution of appropriate concentration. DNA concentrations are in terms of moles of molecules per liter. Samples were incubated at room temperature for ~30 min. A 20 µl aliquot of the mixture was deposited onto freshly cleaved mica and incubated for 15 min in a humidified chamber. For trapping conditions, the mica was first incubated with water for >14 h, rinsed and blown dry (32). Adsorption of the sample to the substrate was as above, except that the final magnesium concentration was reduced to 1 mM and the incubation time on the surface was 1 min. Following incubation, samples were rinsed with a flow of corresponding ethanol/water solution for 3–4 s (~20 ml solution in total), and then rapidly blown dried using a burst of compressed gas (Vari-Air, Peca Products, Janesville, WI).

AFM imaging

A Nanoscope IIIa AFM controller with a Multimode AFM (Digital Instruments, Santa Barbara, CA) was used for imaging. Single crystal silicon cantilevers (Model TESP; Digital Instruments) were cleaned by exposure to high intensity UV light (UVO-Cleaner, Jelight Company Inc., Laguna Hills, CA) for 3 min before use. All AFM imaging was conventional ambient tapping mode AFM, with scan speeds of ~3 Hz and data collection at 512 × 512 pixels. Most of the AFM images were taken at a scan size of 3 µm × 3 µm. Images have inverted contrast for presentation purposes.

Data processing

The AFM images were analyzed using AFMIPS and NIH Image software. The AFMIPS is an image analysis tool developed in our laboratory that can automatically outline DNA molecules and determine their contour lengths (36,37). The AFMIPS was used in a semi-interactive mode where all the outputs from the program were monitored and occasionally checked manually by the operator. For the present work several additional functions were added for the persistence length measurements. To determine the persistence length, the positions of the detected DNA molecules were over-sampled to every 1 nm by linear interpolation. The angle Θ between two adjacent segments along the DNA, each of length *l* from a vertex position, was calculated by using the law of cosines. By incrementing the vertex position along the DNA in steps of length *l*, many angle measurements were obtained and subjected to moment analysis as previously described (38,39). Where needed, hand tracing of DNA molecules was performed using NIH Image (version 1.58).

RESULTS

The experimental approach used here was to examine DNA adsorbed onto a mica surface in the presence of increasing concentrations of ethanol. DNA was incubated with ethanol and magnesium, followed by a rinse with ethanol/water solution only (at the appropriate concentration) and air drying. The rinse was performed without Mg^{2+}, to prevent the formation of salt crystals on the mica surface. These are essentially non-trapping conditions as defined by Rivetti *et al*. (32), and thus the DNA should be free to rearrange on the mica surface after adsorption. We also examined trapping conditions by using proton exchanged mica (39). Rinsing with pure water results in DNA relaxation into all-B-form (Table 1), suggesting that the A-form to B-form transition was very fast. At the lower ethanol concentrations individual DNA molecules were well separated and appeared relaxed (Table 2). As the ethanol concentration increases, the molecules have increasingly complex morphologies, including highly looped structures (flowers) and toroids. In the results presented here we separate single relaxed molecules, defined as a DNA molecule that does not touch another molecule and does not cross itself more than once, from the more complex structures. The contour length and the persistence length of single relaxed molecules are measured as a function of ethanol concentration. The contour length distribution is further analyzed to provide an upper bound to the characteristic domain size during a B-form to A-form transition of the DNA. Finally, a description of the more complex DNA morphologies observed is presented.

Table 1. Effect of the rinse solution on the structure of DNA adsorbed to mica

Initial ethanol concentration (%)	Rinse	Contour length (nm)
5	Water	646 ± 18
	1% ethanol	621 ± 30
	5% ethanol	606 ± 24
30	Water	650 ± 17
	30% ethanol	532 ± 25

All water rinses resulted in DNAs with B-form contour lengths, even after treatment with 30% ethanol.

Table 2. Distribution of extended and looped DNA as a function of ethanol

Ethanol	Single molecules			Multi-molecular aggregates	
(%)	Extended	Single loop	Multi-loop	Small	Large
0	154	12	3	–	–
3	120	19	8	–	–
5	92	38	10	3	–
6	90	25	21	1	–
10	95	29	27	2	–
15	72	43	51	8	–
20	59	44	52	2	2
25	21	25	37	4	4

There is a clear tendency to increasingly looped and complex structures at higher ethanol concentrations. The average loop diameter is 48 nm. Eleven AFM images were examined for each ethanol concentration, with the exception that 25 images were examined for 0% ethanol.

DNA contour length as a function of ethanol concentration

AFM images of the 1968 bp DNA adsorbed at three different concentrations of ethanol are shown in Figure 1, along with the corresponding contour length distribution. In the absence of ethanol, almost all DNA molecules are extended with few

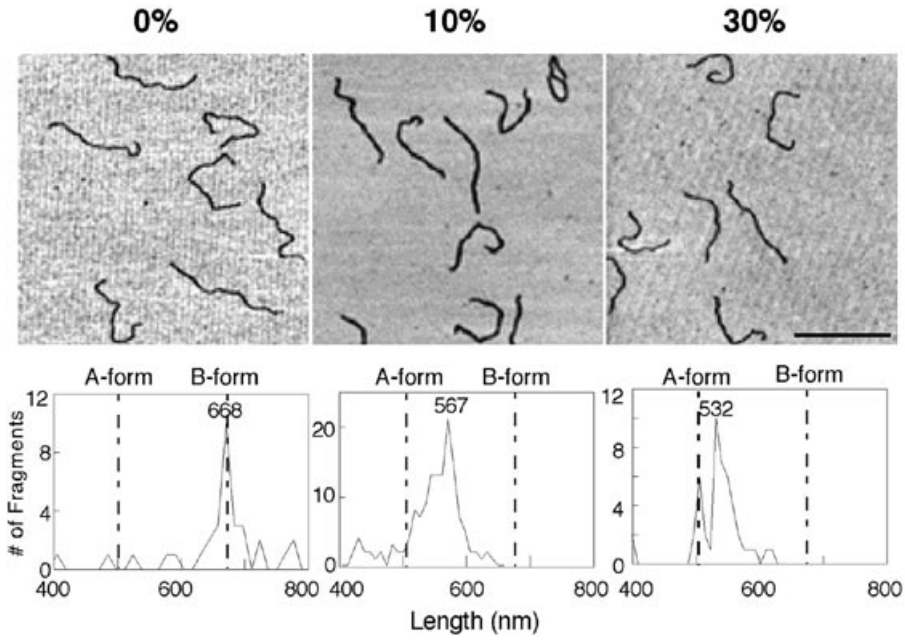

Figure 1. Ethanol induced B-form to A-form transition of DNA on mica. The contour lengths of a 1968 bp DNA fragment adsorbed to mica were shown to depend on the concentration of ethanol in solution. In the absence of ethanol, the DNA has a length that is consistent with an all B-form conformation. In a 10% ethanol solution, the lengths of individual molecules are intermediate to that predicted for all A-form or all B-form suggesting that the molecules are trapped with a mixed composition. At 30% ethanol the contour lengths are consistent with nearly all A-form DNA. Only extended and traceable (one intramolecular loop or less) DNA molecules were counted. Scale bar is 500 nm.

intra-molecular contacts and almost no inter-molecular contacts. The mean contour length, 668 ± 17 nm, is essentially identical to that expected for all-B-form DNA, indicating that DNAs adsorbed on the surface adopt B-form conformation. As the concentration of ethanol is increased to 30%, the mean contour length of DNAs becomes 21% shorter than that in the absence of ethanol. This is consistent with the previous observation by Courey *et al*. (34). This change is very close to that expected for a B-form to A-form transition of DNA, which would be ~23.5% based on the difference in the rise per base pair of 3.4 Å for B-form and 2.6 Å for A-form DNA (1). At the intermediate ethanol concentration the distribution of contour lengths shows that length of individual molecules is intermediate to all-B-form or all-A-form DNA. This suggests that these molecules have been trapped with a mixed composition of A-form and B-form DNA. Results for the 3033 bp DNA were similar.

For a larger series of ethanol concentrations it can be seen that the contour lengths of both the 1968 and 3033 bp DNA decrease monotonically with increasing ethanol concentration (Fig. 2). The lengths appear to approach all A-form DNA above ~25% ethanol, although there is some deviation for the 3033 bp DNA that plateaus at a length slightly larger than all A-form.

Adsorption under certain conditions has been shown to trap DNA polymer chain statistics from solution (32). We examined the effect of ethanol on DNA under these conditions by using proton exchanged mica. Soaking mica in water for >14 h results in the exchange of surface potassium ions with protons. Because the long DNAs used above were highly entangled under trapping conditions and could not be readily traced, a smaller (672 bp) DNA molecule was used. The contour length of this molecule is 230 ± 9 nm in the absence of ethanol, close to B-form. As expected for trapping conditions, there is no significant change in

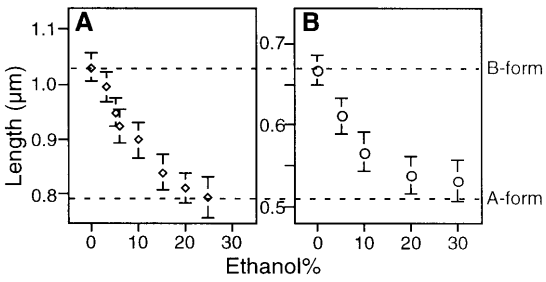

Figure 2. The contour length of the 3033 bp DNA (**A**) and the 1968 bp DNA fragment (**B**) as a function of ethanol concentration. For each data point, about 25 AFM images were subject to length measurements. Only extended and traceable (one intramolecular loop or less) DNA molecules were counted.

contour length up to 25% ethanol (data not shown). Trapping conditions were confirmed by a changes in end-to-end distance measurements, compared to non-trapping conditions.

Estimate of the A-form/B-form domain size

The width of the DNA length distribution at any given ethanol concentration is relatively narrow, typically ~50–60 nm at half height for the 3033 bp DNA. For the non-trapping conditions this provides an opportunity to estimate the size of the A- or B-form domains in the DNA molecules. Using a simple model in which the DNA is composed of a number of equal sized domains that can be either A-form or B-form (Fig. 3A), binomial statistics can be used to estimate the domain size (40). If we begin by dividing a DNA molecule into N segments,

$$N = n_a + n_b \quad \mathbf{1}$$

Here n_a and n_b refer to the number of A-form and B-form domains, respectively. If the domain size is *d* bp, the contour length of the molecule (L), in nanometers, is:

$$L = (0.26n_a + 0.34n_b)d \quad \mathbf{2}$$

For the 3033 bp fragment, we have:

$$n_b = (3033 - n_a d)/d \quad \mathbf{3}$$

Substituting into equation **2**, we obtain:

$$n_a = (1031 - L)/(0.08d) \quad \mathbf{4}$$

Then from binomial statistics the probability function of a domain being A-form, $H_N(n_a)$, is:

$$H_N(n_a) = \binom{N}{n_a} P_a^{n_a} (1 - P_a)^{N - n_a}, \quad n_a = 0, 1, 2, ...N \quad \mathbf{5}$$

Here P_a is the probability that any single domain will be A-form. This value is obtained from the center of the length distribution histogram relative to full A-form or B-form DNA. When the length distribution is half way between the two, $P_a = P_b = 0.5$. The center position of the length distribution also constrains the relationship between N and n_a, and for $P_a = 0.5$ the ratio of n_a to N is 0.5. By fitting the experimental length distribution $H_N(n_a)$ to equation **5**, we obtain the total number of domains, and thereby obtain the domain size (Fig. 3B). The domain size for the 3033 bp DNA is 54 ± 3 bp, and appears to be independent on the ethanol concentration in the range 3–15%.

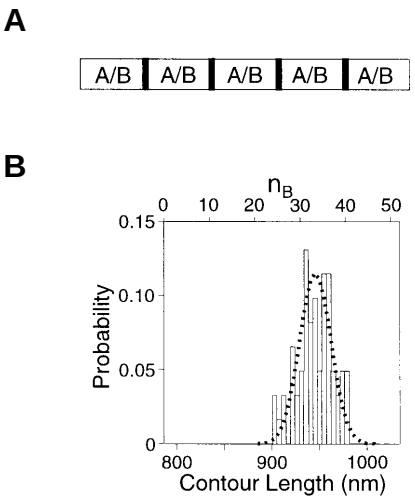

Figure 3. Estimation of the A/B domain size from a simple binomial model. (**A**) In this model the DNA is composed of an unknown number (N) of equal size domains, that can be either all-A-form or all-B-form. The junction between two domains is considered negligible. (**B**) Example of the fitting of the binomial model (equation **5**; dotted line) to data for the distribution of the contour lengths of the 3033 bp DNA (box histogram) at 10% ethanol. The total domain obtained is 58, 58, 53, 52, 58 and 59 for the DNA in the presence of 3, 5, 6, 10, 15 and 20% ethanol, respectively. Thus the average domain size is 54 bp. Because there are measurement errors that contribute to the width of the histogram, this domain size estimate represents an upper limit.

Persistence length as a function of ethanol concentration

The apparent persistence length of DNA on the mica can be determined from AFM images of individual DNA molecules (32). Here we used the approach described by Frontali *et al.* (38), who showed that persistence length can be determined by measuring the dependence of the angle Θ between two segments (at an arbitrary position on the molecule) on the length of the segments *l*. For the 3033 bp DNA fragment, the mean Θ as a function of separation distance *l* in the presence of different ethanol concentrations is shown in Figure 4A. Moment analysis of that data shows that the apparent persistence lengths decrease monotonically as the concentration of ethanol increases (Fig. 4B). Similar results are obtained for the 1968 bp DNA fragment (Fig. 4C).

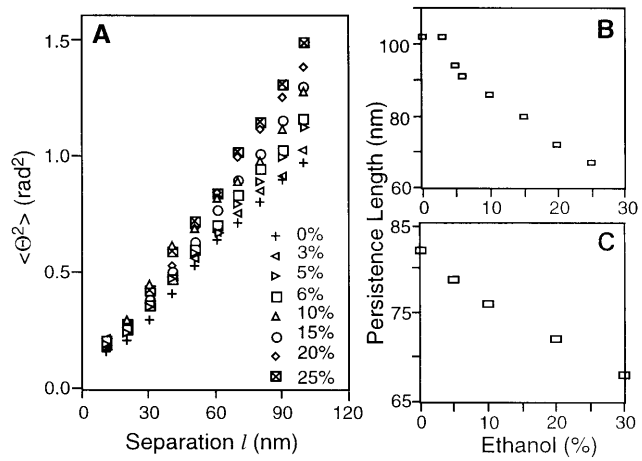

Figure 4. Effect of ethanol on apparent persistence length of DNA. Apparent persistence length of DNA as a function of ethanol. (**A**) Data used to determine persistence lengths. The dependence of the angle Θ between two adjacent segments on the separation distance *l* for several ethanol concentrations. The persistence length of (**B**) the 3033 bp DNA and (**C**) the 1968 bp DNA as a function of ethanol concentration.

Morphological characterization

In the absence of ethanol, individual DNA molecules are well separated on the surface, and have a relaxed morphology. However, as the ethanol concentration is increased, a range of more complex structures appears. At any particular ethanol concentration above a few percent there are often a number of structural forms; however, there is a general tendency for the structures to become more complex with increasing ethanol concentration (Fig. 5). At ethanol concentrations <15% there are few intermolecular contacts, but individual molecules have an increased number of intramolecular contacts as determined from the number of intramolecular loops, as a function of increasing ethanol concentrations (Table 2). At ethanol >15%, multi-molecular complexes appear, including ones with the flower shaped appearance recently described for spermidine induced DNA condensation (Fig. 5). These flowers are highly looped with one or few crossover points. The individual crossovers can have tens of DNA strands. At the highest concentrations of ethanol used we find toroidal structures. These toroids are 50–100 nm in diameter, and are up to 5 nm tall (Fig. 6). It should be noted that despite the tendency for increasing complexity with increasing ethanol concentration, the structures at any given ethanol concentration are highly polymorphic. For example, at 35% ethanol, the structure of DNA molecules was found ranged from completely extended to almost complete toroids (Fig. 6).

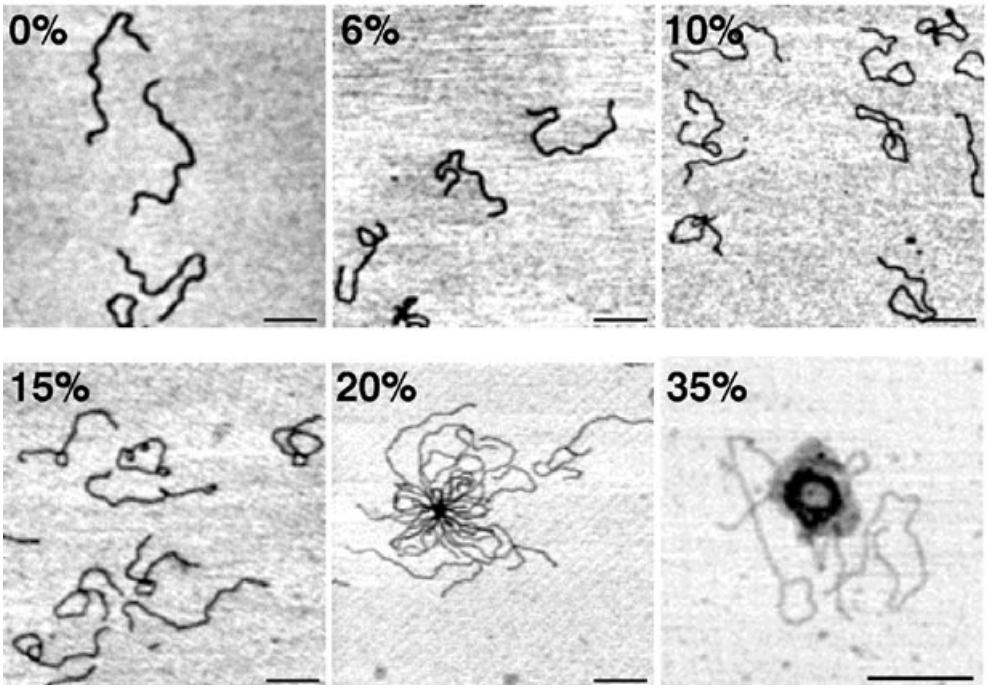

Figure 5. Typical AFM images of the 3033 bp DNA at different ethanol solutions. At increasing ethanol concentration there is a general tendency for increasingly looped and complex structures. Highly complex structures, such as the toroids, were very rare. Although they were only found at the highest ethanol concentrations. Scale bar is 250 nm for all images.

DISCUSSION

B–A transition at low ethanol concentrations

In solution, an ethanol concentration in the range 70–85% is needed to shift the DNA conformation from B-form to A-form (2–6). Corey *et al*. have previously reported that mica facilitates the B–A transition, and that at 30% ethanol the DNA is all A-form (34). Here we confirm that observation under conditions where the DNA molecule is adsorbed but not trapped on the surface, and show that this transition proceeds through molecules that appear to be mixed A-form and B-form. Under adsorption conditions where the polymer chain statistics are trapped there is no transition, as would be predicted given the high ethanol concentrations required for the B-form to A-form transition in solution. In our analysis of the contour lengths we make two assumptions; DNA in the absence of the ethanol is B-form, and that DNA has a contour length of 2.6 Å/bp indicates A-form DNA. Because the contour length of C-form DNA is very close to that of B-form, it is possible that there are transitions between B-form and C-form that we do not detect. It is also possible that the unique conditions near the surface give rise to some yet unidentified form of DNA with the appropriate contour length. We have not examined the kinetics of the B–A transition in this system, so at present we can only conclude that the mica must stabilize A-form DNA in the presence of ethanol and magnesium. The mechanism by which this occurs is not known. We note that it has been reported that for DNA fibers Mg^{2+} stabilizes the B-form of DNA in the presence of ethanol up to 50–70%, and thus disfavors the B-A transition (6). However, the concentration of Mg^{2+} at the mica/solution interface should be >0.4 M (41), which is significantly higher than concentrations used in other studies. Such a high concentration of Mg^{2+} would reduce the local water activity and hence could act to dehydrate the DNA and thus stabilize the A-form.

The DNA molecules with lengths intermediate to all A-form and all B-form must have a mixed composition of A- and B-form. Intuitively one might have thought that air drying the samples would have caused all the DNA to become A-form. We suggest two possible reasons why this does not occur; the DNA–mica interactions are sufficiently strong to prevent this transition on the time scale of drying or the B-to-A transition is very slow on the time scale of drying. In either case, we assume that once the molecules are dry, they are trapped in forms that represent their lengths prior to drying. It is reasonable to assume that there are domains with some characteristic size. While the nature of those domains is not well understood, some insights can be had from a simple binomial model in which the DNA molecule is composed of a series of equal sized domains with a probability of being A-form or B-form determined by the ethanol concentration. Using such a model we estimate the domain size to be <54 bp. The model assumes that the junction between A-form and B-form DNA is infinitely small, and that there are no experimental errors in the length measurements. However, because the junction must have some finite number of bases, and there must be experimental errors in the length measurements, this domain size estimate is an upper bound. It is thus in reasonable agreement with other estimates of the domain size, which range from 10 to 30 bp for the ethanol-induced DNA B–A transitions in solution (2,7,8).

Apparent persistence length decreases with increasing ethanol concentration

For the DNA molecules of 3033 and 1968 bp used here, the apparent persistence length in the B-form is ~103 and 82 nm,

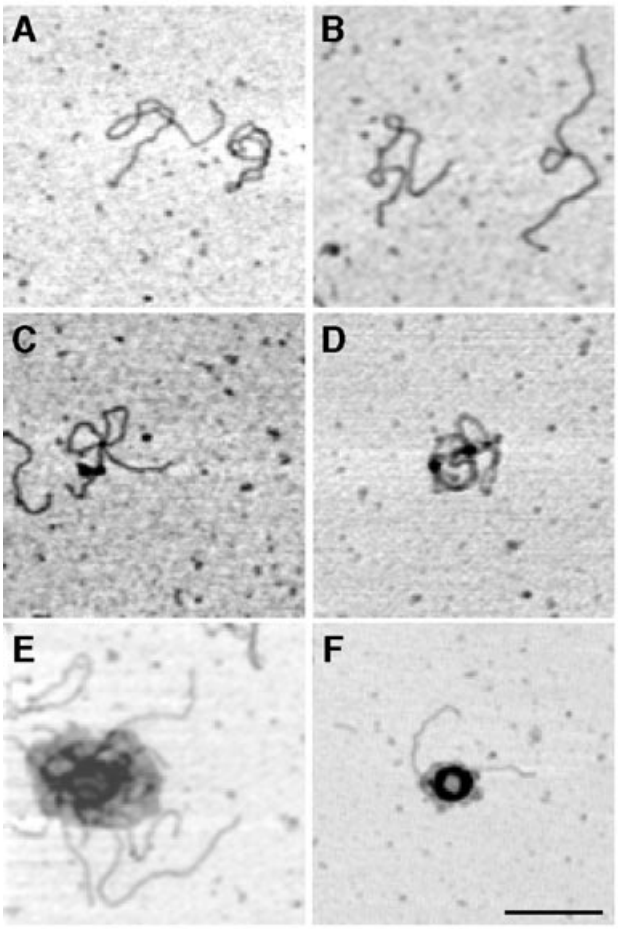

Figure 6. Range of intermediates of condensed DNA at 35% ethanol. A very wide range of structures is seem at any given ethanol concentration, particularly at the higher concentrations. Scale bar is 250 nm for all images.

respectively. These values are larger than the commonly reported value of 50 nm due to excluded volume effects for these relatively large DNA molecules (39). As the ethanol concentration increases, the apparent persistence length of DNA fragments on the mica surface decreases monotonically when the lengths are expressed in terms of distance. However, expressed in terms of base pairs the measured persistence length is roughly constant (~250 bp) during the ethanol induced B-form to A-form transition. This is quite different than the B-form to A-form transition in solution, which is accompanied by a 3-fold increase in persistence length from 50 nm for B-form to 150 nm for A-form (4-fold increase in terms of base pairs) (42). Thus, under the conditions used here, there appears to be a relative decrease in the stiffness of the DNA, or an increase in the intrinsic bending of the molecules. It is also possible that the different water activities change self-exclusion properties, which could result in a reduction of persistence length at higher ethanol concentrations. The fact that increasingly looped structures form at higher ethanol concentrations suggests that there is in fact increased bending of the DNA.

Structure of ethanol-induced DNA condensates

As discussed above, a transition from B-form to A-form DNA is one of the early events in response to added ethanol. In addition, there is a general tendency for increasingly looped and complex structures with increasing ethanol concentration. At the higher ethanol concentrations we observed some well-defined DNA structures that are very similar to structures previously described. These include toroids, which can be formed by simple mixing of a dilute DNA solution with a multivalent cation such as spermidine (43–45) or $Co(NH_3)_6^{3+}$ (46), or introducing ethanol into a DNA solution (11,13,14), and flowers which are formed on the surface of mica in the presence of spermidine (35) or other multivalent cations (47). Because of the appearance of toroids at the highest ethanol concentrations, it is tempting to speculate that the structures seen at lower concentrations are intermediates in the condensation pathway. However, the coexistence of many different structures at any given ethanol concentration makes it difficult from the present data to definitely determine the order in which the structures appeared. Despite this the data suggest that the structural changes begin with the formation of intramolecular loops, followed by multi-molecular looped structures (flowers) and toroids. This series of structural changes is similar to that recently reported for spermidine induced DNA condensation on the surface of mica, with the exception that in the spermidine experiments complete toroids were not formed (35). The lack of toroids in those experiments was attributed to problems with higher concentrations of spermidine interfering with AFM imaging. Hence the present results provide a link between flowers and toroids of the type that have been well characterized in solution. There are a number of potential concerns with interpretation of the type of data presented here, including the influence of the substrate, sampling and drying. These issues were recently discussed in some detail for the case of spermidine induced DNA condensation on mica (35).

CONCLUSION

DNA molecules confined to a mica surface in the presence of Mg^{2+} undergo a cooperative B–A transition induced by low concentrations of ethanol. At higher ethanol concentrations, toroid DNA condensation follows the complete B–A transition. The ethanol-induced DNA condensation on surface shares similar structural intermediates with the spermidine-induced condensation.

ACKNOWLEDGEMENTS

We thank Dr Qi-Chun Tang of the Johns Hopkins University School of Medicine for providing the linear 1968 bp DNA used. This work was supported by NIH grants HGO1518 (J.H.H.), and internal research and development funds from the Johns Hopkins University Applied Physics Laboratory (T.S.S.).

REFERENCES

1 Saenger,W. (1984) *Principles of Nucleic Acids Structure*. Springer-Verlag, New York.
2 Ivanov,V.I. and Krylov,D. (1992) *Methods Enzymol.*, **211**, 111–127.
3 Cheatham,T.E.,III, Crowley,M.F., Fox,T. and Kollman,P.A. (1997) *Proc. Natl Acad. Sci. USA*, **94**, 9626–9630.
4 Ivanov,V.I., Minchenkova,L.E., Minyat,E.E., Frank-Kamenetskii,M.D. and Schyolkina,A.K. (1974) *J. Mol. Biol.*, **87**, 817–833.
5 Rupprecht,A., Piskur,J., Schultz,J., Nordenskiold,L., Song,Z. and Lahajnar,G. (1994) *Biopolymers*, **34**, 897–920.
6 Schultz,J., Rupprecht,A., Song,Z., Piskur,J., Nordenskiold,L. and Lahajnar,G. (1994) *Biophys. J.*, **66**, 810–819.
7 Minchenkova,L.E., Schyolkina,A.K., Chernov,B.K. and Ivanov,V.I. (1986) *J. Biomol. Struct. Dyn.*, **4**, 463–476.

8 Ivanov,V.I., Minchenkova,L.E., Burckhardt,G., Birch-Hirschfeld,E., Fritzsche,H. and Zimmer,C. (1996) *Biophys. J.*, **71**, 3344–3349.
9 Becker,M.M. and Wang,Z. (1989) *J. Biol. Chem.*, **264**, 4163–4167.
10 Bloomfied,V.A. (1996) *Curr. Opin. Struct. Biol.*, **6**, 331–341.
11 Arscott,P.G., Ma,C., Wenner,J.R. and Bloomfield,V.A. (1995) *Biopolymers*, **36**, 345–364.
12 Flock,S., Labarbe,R., and Houssier,C. (1996) *Biophys. J.*, **70**, 1456–1465.
13 Lang,D. (1973) *J. Mol. Biol.*, **78**, 247–254.
14 Lang,D., Taylor,T.N., Dobyan,D.C. and Gray,D.M. (1976) *J. Mol. Biol.*, **106**, 97–107.
15 Eickbush,T.H. and Moudrianakis,E.N. (1978) *Cell*, **13**, 295–306.
16 Fang,Y. and Yang,J. (1997) *J. Phys. Chem. B*, **101**, 441–449.
17 Fang,Y. and Yang,J. (1997) *J. Phys. Chem. B*, **101**, 3453–3456.
18 Lasic,D.D. (1997) *Liposomes in Gene Delivery.* CRC Press, Boca Raton, FL, pp. 113–143.
19 van Holde,K.E. (1988) *Chromatin.* Springer-Verlag, New York.
20 Wang,B.C., Rose,J., Arents,G. and Moudrianakis,E.N. (1994) *J. Mol. Biol.*, **236**, 179–188.
21 Arents,G. and Moudrianakis,E.N. (1995) *Proc. Natl Acad. Sci. USA*, **92**, 11170–11174.
22 Han,W., Lindsay,S.M., Dlakic,M. and Harrington,R.E. (1997) *Nature*, **386**, 563.
23 Han,W., Dlakic,M., Zhu,Y.J., Lindsay,S.M. and Harrington,R.E. (1997) *Proc. Natl Acad. Sci. USA*, **94**, 10565–10570.
24 Pfannschmidt,C. and Langowski,J. (1998) *J. Mol. Biol.*, **275**, 601–611.
25 Erie,D.A., Yang,G., Schultz,H.C. and Bustamante,C. (1994) *Science*, **266**, 1562–1566.
26 Rippe,K., Guthold,M., von Hippel,P.H. and Bustamante,C. (1997) *J. Mol. Biol.*, **270**, 125–138.
27 Bustamante,C., Vesenka,J., Tang,C.L., Rees,W., Guthold,M. and Keller,R. (1992) *Biochemistry*, **31**, 22–26.
28 Fang,Y. and Hoh,J.H. (1998) *Nucleic Acids Res.*, **26**, 588–593.
29 Lyubchenko,Y.L., Gall,A.A., Shlyakhtenko,L., Harrington,R.E., Jacobs,B.L., Oden,P.I. and Lindsay,S. (1992) *J. Biomol. Struct. Dyn.*, **10**, 589–606.
30 Yang,J., Takeyasu,K. and Shao,Z. (1992) *FEBS Lett.*, **301**, 173–176.
31 Yoshida,K., Yoshimoto,M., Sasaki,K., Ohnishi,T., Ushiki,T., Hitomi,J., Yamamoto,S. and Sigeno,M. (1998) *Biophys. J.*, **74**, 1654–1657.
32 Bustamante,C. and Rivetti,C. (1996) *Annu. Rev. Biophys. Biomol. Struct.*, **25**, 395–429.
33 Hansma,H.G. and Hoh,J.H. (1994) *Annu. Rev. Biophys. Biomol. Struct.*, **23**, 115–139.
34 Coury,J.E., Anderson,J.R., McFail-Isom,L., Williams,L.D. and Bottomley,L.A. (1997) *J. Am. Chem. Soc.*, **119**, 3792–3796.
35 Fang,Y. and Hoh,J.H. (1998). *J. Am. Chem. Soc.*, **120**, 8903–8909.
36 Fang,Y., Spisz,T.S., Wiltshire,T., D'Costa,N.P., Bankman,I.N., Reeves,R.H. and Hoh,J.H. (1998) *Anal. Chem.*, **70**, 2123–2129.
37 Spisz,T.S., Fang,Y., Seymour,C.K., Reeves,R.H., Hoh,J.H. and Bankman,I.N. (1998) *Med. Biol. Eng. Comp.*, **36**, 667–672.
38 Frontali,C., Dore,E., Ferrauto,A. and Gratton,E. (1979) *Biopolymers*, **18**, 1353–1373.
39 Rivetti,C., Guthold,M. and Bustamante,C. (1996) *J. Mol. Biol.*, **264**, 919–932.
40 Yeargers,E.K., Shonkwiler,R.W. and Herod,J.V. (1996) *An Introduction to the Mathematics of Biology with Computer Algebra Models.* Birkhouser, Boston, MA.
41 Pashley,R.M. and Israelachvili,J.N. (1984) *J. Colloid Interface Sci.*, **97**, 446–455.
42 Charney,E., Holly-Ho,C. and Rau,D.C. (1991). *J. Biomol. Struct. Dyn.*, **9**, 353–362.
43 Chattoraj,D.K., Gosule,L.C. and Schellman,J.A. (1978) *J. Mol. Biol.*, **121**, 327–337.
44 Gosule,L.C. and Schellman,J.A. (1976) *Nature*, **259**, 333–335.
45 Lin,Z., Wang,C., Feng,X., Liu,M., Li,J. and Bai,C. (1998) *Nucleic Acids Res.*, **26**, 3228–3234.
46 Widom,J. and Baldwin,R.L. (1983) *Biopolymers*, **22**, 1595–1620.
47 Hansma,H.G., Golan,R., Hsieh,W., Lollo,C.P., Mullen-Ley,P. and Kwoh,D. (1998) *Nucleic Acids Res.*, **26**, 2481–2487.